Available online at www.sciencedirect.com
ScienceDirect
Surface Science 601 (2007) 425–433
SURFACE SCIENCE
www.elsevier.com/locate/susc

Profile imaging of reconstructed polar and non-polar surfaces of ZnO

Yong Ding, Zhong Lin Wang *

School of Materials Science and Engineering, Georgia Institute of Technology, Atlanta, GA 30332-0245, United States

Received 5 May 2006; accepted for publication 26 July 2006
Available online 10 November 2006

Abstract

The atomic scale surface structures of ZnO $(01\bar{1}0)$ non-polar as well as $(0\bar{1}11)$ and $\pm(0001)$ polar surfaces have been directly imaged by high-resolution transmission electron microscopy (HRTEM). The observations were made on clean surfaces created by irradiating a single ZnO nanobelt using 400 keV electron beam in TEM, under which ZnO dots were grown epitaxially and in situ on the surface of the nanobelt. A technique is demonstrated for directly distinguishing the surface polarity of the $\pm(0001)$ polar surfaces. For the $(01\bar{1}0)$ non-polar surface, HRTEM images and simulation results indicate that the Zn ions in the first and second layer suffer from inward and outward relaxation, respectively; the oxygen ions in the first and second layer prefer shifting to vicinal Zn ions to shorten the bonding distance. For the oxygen-terminated $(0\bar{1}11)$ polar surface, the oxygen ions at the outmost top layer were directly imaged. a $\times 2$ reconstruction has also been observed at the $(0\bar{1}11)$ surface, and its atomic structure has been proposed based on image simulation. Oxygen-terminated $(000\bar{1})$ polar surface is flat and shows no detectable reconstruction. For the Zn-terminated (0001) polar surface, HRTEM may indicate the existence of Zn vacancies and a possibly *c*-axis, random outward displacement of the top Zn ions. Our data tend to support the mechanism of removal of surface atoms for maintaining the stability of (0001) polar surfaces.

Keywords: Surface structure; High-resolution transmission electron microscopy; Profile image; Zinc oxide; Polar surface

1. Introduction

ZnO is an interesting and important II–VI semiconductor for both applications and basic researches owing to its unique physical and chemical properties [1]. The electronic properties of the ZnO surfaces are particularly important for its application as chemical and gas sensor as well as catalyst for hydrogenation and dehydrogenation [2,3]. More importantly, ZnO has attracted considerable attention in nanotechnology for the unique structures and devices that it has offered [4–8]. For the ZnO nanostructures, with the increased surface-to-bulk ratio, the effect played by the surfaces, especially the polar surfaces, is critically important. As a result, various polar surface dominated nanostructure [9] such as nanobelts [10], nanorings [11], nanosprings [12,13], and nanohelices [14], have been found for wurtzite ZnO. The formation mechanism was attributed to the minimization of electrostatic interaction energy contributed by the ionic charges on the polar surfaces.

From the crystal structural point of view, ZnO takes the hexagonal wurtzite structure with space group as $P6_3mc$ [15]. Close-packed oxygen and zinc layers stack along the *c*-axis with alternating distances 0.69 Å and 1.99 Å, respectively [16]. The exposed (0001) and $(000\bar{1})$ surfaces are composed uniquely by Zn^{2+} and O^{2-} ions, respectively, to form polar surfaces, while $\{01\bar{1}0\}$ surfaces perpendicular to the *c*-axis are composed by Zn–O dimers with neutral charge, forming the non-polar surfaces. The dangling bonds on such surfaces make the system unstable [17]. It was considered that the Zn–O surface dimers on non-polar $(01\bar{1}0)$ surface are energetically favorable after a slight tilting and an inward displacement into the volume [18]. However, the detailed configuration

* Corresponding author. Tel.: +1 404 894 8008; fax: +1 404 894 9145.
E-mail addresses: yong.ding@mse.gatech.edu (Y. Ding), zhong.wang@mse.gatech.edu (Z.L. Wang).

0039-6028/$ - see front matter © 2006 Elsevier B.V. All rights reserved.
doi:10.1016/j.susc.2006.07.063

about the relaxation of the surface atoms is still controversial [19,20]. Furthermore, in contrast to most known oxides with polar surfaces, ZnO $\pm(0001)$ polar surfaces are quite stable without faceting or exhibiting massive surface reconstructions [21–23]. Electrostatic consideration as well as electronic structure calculation suggests that a rearrangement of charges on both outmost layers of a ZnO crystal may cancel the polarity [24]. The reduced surface charge density may occur through three possible mechanisms: (1) creation of surface state and transfer of negative charges from oxygen sites to Zn sites; (2) removal of surface atoms and (3) presence of positively or negatively charged impurity atoms on the oxygen or Zn-terminated surfaces [16]. It is still being debated which mechanism is the dominant one.

Many works have been carried out to investigate ZnO surface reconstruction and the electronic structure by first principle calculations [25–29] and low-energy positron diffraction [30], reflection high-energy electron diffraction (RHEED) [31], low-energy electron diffraction (LEED) [32], electron energy-loss spectroscopy (EELS) [33], He-atom scattering [34], surface X-ray diffraction [20], scanning tunneling microscopy (STM) [35], and more [36–38]. Considering that high-resolution transmission electron microscopy (HRTEM) can provide real-space information about surface steps, terraces, and defects at atomic resolution, and it has been successfully applied in the study of surface reconstruction of many materials, such as CdTe and silicon [39–41], in this paper, we use HRTEM to study the reconstruction of clean ZnO surfaces formed in situ in TEM. By comparing the experimental images with simulated images based on the proposed models, the reconstruction and relaxation of surface atoms have been identified, providing direct evidence about the structural configuration of surface atoms.

2. Experimental

The original sample was from the ZnO nanobelts prepared by a technique reported previously [10]. The suspended nanobelt has a growth direction of $[01\bar{1}1]$ with large top and bottom surfaces of $\pm(2\bar{1}\bar{1}0)$ (Fig. 1). By irradiating a ZnO nanobelt with a 400 keV electron beam in a JEOL 4000EX HRTEM, ZnO quantum dots of ~5 nm in size with clean surfaces were formed in situ epitaxially on the ZnO nanobelt surfaces, as shown at the lower bottom part of the TEM image presented in Fig. 1. The thickness of the quantum dots (QDs) is less than 3 nm and the surface is clean as formed in situ in an environment of 10^{-8} Torr, providing an ideal sample for profile imaging of its surfaces. The HRTEM images of the ZnO quantum dots were recorded with the electron beam along $[2\bar{1}\bar{1}0]$. The experimentally recorded images were compared to the simulated images for quantifying the surface reconstruction. The image simulation and processing were done using *Cerius2* [42] and Gatan Digital Micrograph software, respectively.

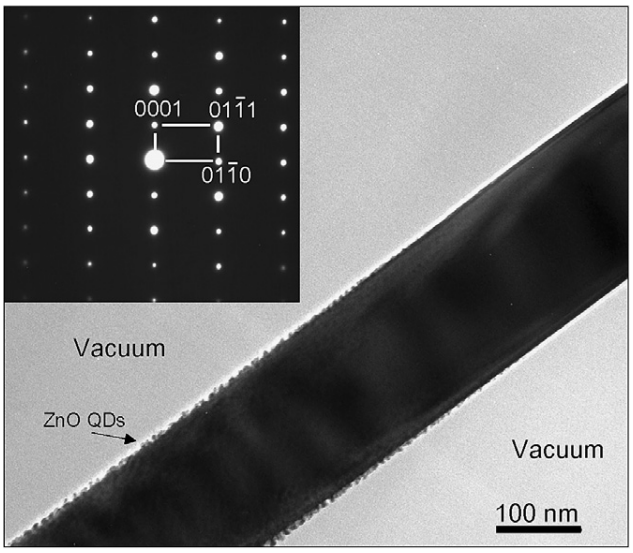

Fig. 1. TEM image and electron diffraction pattern of a ZnO belt, which is suspended in vacuum. The electron beam irradiation induced quantum dots can be seen at the belt side surfaces.

3. Results and discussion

For the understanding of the observed data, the atomic structure of ZnO is described in Fig. 2, where the left- and right-hand sides correspond to the projections of the atomic model along $[2\bar{1}\bar{1}0]$ and [0001] directions, respectively. Three types of surface plane are emphasized in Fig. 2, $(01\bar{1}0)$, $\pm(0001)$ and $\pm(0\bar{1}11)$. The non-polar $(01\bar{1}0)$ surface is composed of Zn–O dimers. The oxygen-terminated polar surfaces are $(000\bar{1})$ and $(0\bar{1}11)$, and the Zn-terminated polar surfaces are (0001) and $(01\bar{1}\bar{1})$. To investigate the reconstructions of polar surfaces, the first step is to identify the Zn-terminated (0001) and the oxygen-terminated $(000\bar{1})$. In general, converged-beam electron diffraction (CBED) pattern has been used to identify the polarity of ZnO nanobelts [43,44], but CBED works only when the sample thickness is rather thick in the range

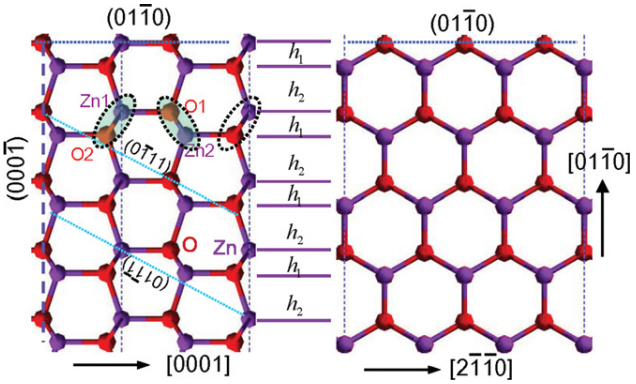

Fig. 2. Left-hand and right-hand sides are the ZnO atomic model projected along $[2\bar{1}\bar{1}0]$ and [0001] directions, respectively. The $(01\bar{1}0)$ non-polar surface, $\pm(0\bar{1}11)$ and $\pm(0001)$ polar surfaces are displayed.

of >100 nm, which is too thick for HRTEM imaging. For the purpose of this study, we must find a way of identifying the polarity for samples of thinner than 5 nm.

3.1. Identification of the polar direction [0001]

By carefully examining the atomic model shown in Fig. 2 and high quality HRTEM images recorded along $[2\bar{1}\bar{1}0]$ in Fig. 3, we found a way of uniquely identifying the positive *c*-axis in the HRTEM images. Fig. 3a and b are two experimental HRTEM images recorded from the two side surfaces of the same belt shown in Fig. 1. The top surface in Fig. 3a and the bottom surface in Fig. 3b belong to $\{01\bar{1}0\}$ family planes. The polar direction should be along horizontal direction. Based on the model shown in Fig. 2, the ideal projected distance between Zn1 and O2, O1 and Zn2 is $a/\sqrt{6} \approx 1.33$ Å which is beyond the resolution limit of the HRTEM (~1.7 Å). But the distance between the Zn1 and O1 atoms is $0.3826c \approx 1.99$ Å, within the resolution power of the microscope. It means that the Zn1 and O1 can have separated contrast in the HRTEM images, while Zn1–O2 and O1–Zn2 dimers will just show a connected contrast like the distorted dark rods displayed in the images in Fig. 3, which were recorded under Scherzer focus.

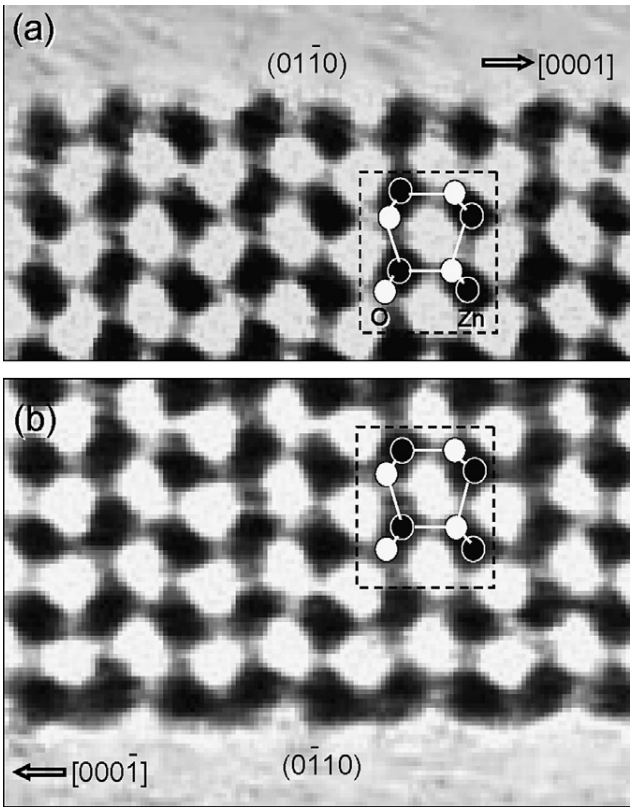

Fig. 3. (a) and (b) are two HRTEM images recorded from the top and bottom side surfaces of the belt shown in Fig. 1. The incident electron beam is along ZnO $[2\bar{1}\bar{1}0]$ direction.

In the experimental HRTEM images in Fig. 3, the centers of the two nearby dark rods are located at the two sides of a horizontal line parallel to the $(01\bar{1}0)$ surface. With considering the different scattering powers of heavy atom Zn and light atom O in mind, each of these dark rods are formed by a Zn–O dimer, the two Zn atoms in the two nearby dimers like the Zn1 and Zn2 shown in Fig. 2, are not aligned along a horizontal line parallel to $(01\bar{1}0)$ plane, the contrast in the dark rods mostly comes from the heavy Zn atom, but the O does introduce a longer tail. Using this phenomenon, we can uniquely identify the Zn and oxygen sites in each dark rod or dimer as indicated by the inserted atomic model. For the Zn–O dimer, if we define the Zn site to be the head and O being the tail, then the two adjacent dimers parallel to $(01\bar{1}0)$ are oriented upward but towards each other with a head-to-tail configuration. In reference to the atomic model shown in Fig. 2, it is clear that the head-to-tail direction is the [0001]. Using this method, the polar directions [0001] in Fig. 3a and b has been marked. Fig. 3a and b should have the same polar direction for they were recorded from opposite surfaces of the same belt as shown in Fig. 1. The determination of positive and negative [0001] directions makes the investigation on the reconstructions of oxygen and Zn-terminated polar surfaces possible. We need to emphasize that the quality of the recorded HRTEM images is critical to the polar direction identification; a small angle misalignment of the crystal can blur out the image and make it ambiguous for determining the polar direction.

3.2. The non-polar $(01\bar{1}0)$ surface

Fig. 4a is a duplication of Fig. 3a, in which some centers of the dark rods are marked by "+". The two different distances h_1' and h_2' between the dark rod centers along $[01\bar{1}0]$ direction have been labeled in Fig. 4a. As mentioned above, the short dark rods also contain the contribution from oxygen ions. Therefore, the planar distance h_1' in Fig. 4a is smaller than h_1 as denoted in Fig. 2, while h_2' is larger than h_2 as denoted in Fig. 2. The smaller distance h_1' at surface compared to those underneath the surface and in the volume shows the possibility of surface reconstruction. The first layer Zn ions moving inward, the Zn ions in the second layer moving outward, or the combination of above two movements are the possibilities of the reconstruction. In order to clarify the detailed reconstruction configuration, HRTEM simulation has been carried out. The simulation conditions were sample thickness of 21.66 Å and Scherzer defocus: −286.7 Å, and Cs = 0.5 mm. The best matched simulation result shown in Fig. 4b was based on the atomic model shown in Fig. 4c, in which the Zn ions located in the first layer move inward and the Zn ions in the second layers move outward as the vertical arrowheads indicated. Such relaxation can give smaller h_1 and larger h_2 (planar distance) among the first three atomic layers.

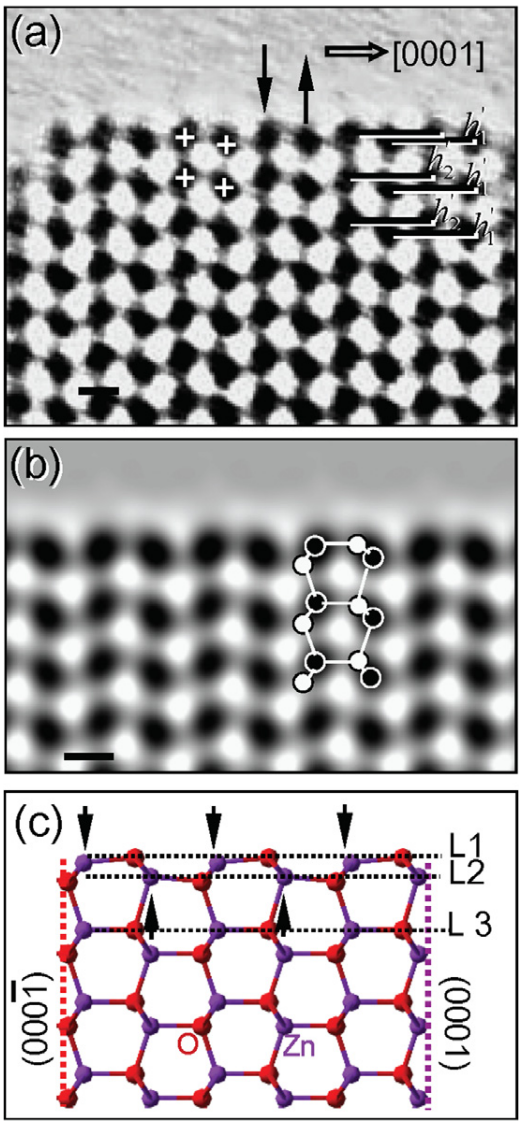

Fig. 4. (a) Duplicated image of Fig. 3a and b simulated HRTEM profile images. The atomic model used for the image simulation is displayed in (c). The scale bars correspond to 5 Å.

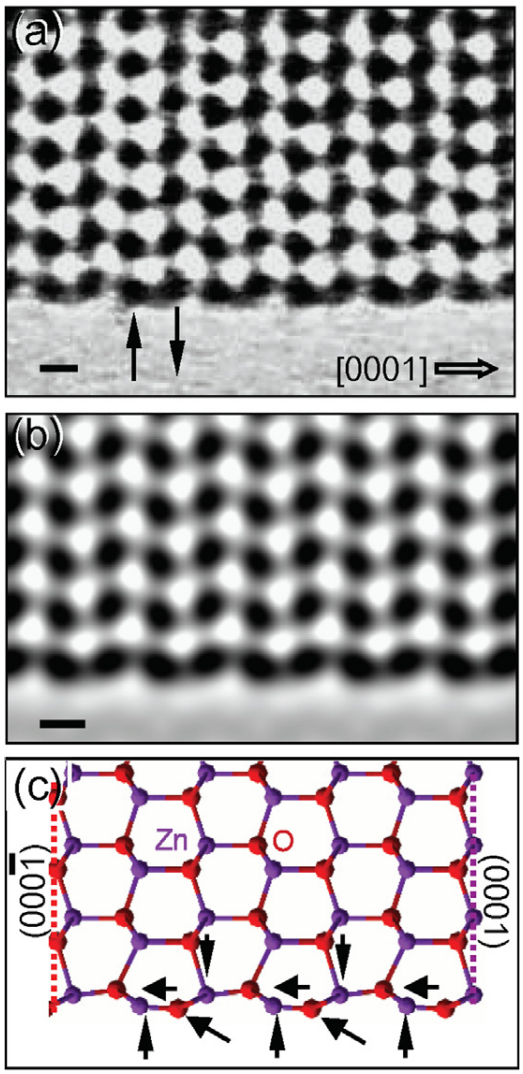

Fig. 5. (a) Duplicated image of Fig. 3b and (b) simulated HRTEM profile image based on the model displayed in (c). The scale bars correspond to 5 Å.

Compared the HRETM images in Fig. 3a and b, the two dark short rods of the Zn–O dimers at the surfaces are well separated in Fig. 3a but not in Fig. 3b. Two reasons may account for such a contrast change, crystal tilting and a shrinking in bonding distance for the Zn head and O tail dimer. The well-separated dark short rods in the volume rule out the first possibility. Based on the assumption of shrunk bonding distance for the Zn–O surface dimers, the modified surface relaxation model is depicted in Fig. 5c. Not only the Zn ions, but also the O ions in the first and second layer shift away from the ideal positions. Arrowheads in Fig. 5c denote the shifting orientation of each surface ion. The best match between the simulated image displayed in Fig. 5b and the experimental image in Fig. 5a, which is a duplicated image of Fig. 3b, supports our assumption.

Based on the best fitted model in Fig. 5c, the displacement of the Zn ions in the first and second surface layer can be estimated as -13% (inward) and 17% (outward) of $d_{(01\bar{1}0)}$. The [0001] direction displacement of the O at surface can be estimated to be $0.1c \sim 0.5$ Å based on the simulated image. Because of the instrument resolution and the difficulty in locating the dark centers in the HRTEM images, the displacement of the relaxed ions may suffer from larger error, but the inward and outward movement of the Zn ions located in the first and second surface layers is confirmed. Our experimental results can help to build reasonable model for future theoretical calculation. In our HRTEM images of $(01\bar{1}0)$ non-polar surface, there is no detectable relaxation beneath the second Zn–O surface layer.

From experimental point of view, only the relaxations of Zn and O ions in the first layer of $(01\bar{1}0)$ non-polar surface

were reported in the literatures. Duke et al. [18] concluded from their best LEED analysis that the first layer Zn ions were displaced downwards by -0.45 ± 0.1 Å and the first layer O^{2-} by -0.05 ± 0.1 Å. The inward displacement of first layer Zn ions observed by Göpel et al. [19] was -0.4 Å in an angle-resolved photoemission experiment. In contrast Jedrecy et al. [20] found that the inward displacement of the first layer Zn ions was only -0.06 ± 0.02 Å after fitting their grazing incidence X-ray diffraction (GIXD) data. From the theoretical point of view, Wang and Duke [45] found a large displacement of Zn of -0.57 Å, while Ivanov and Pollmann [28] obtained no displacement. The calculation based on shell model [46] predicted the displacement of Zn in the first layer and second layer were -0.25 Å and 0.165 Å, respectively. The density-functional study by Meyer and Marx [25] gave the displacement of Zn in the first layer being -0.36 Å.

Different from the techniques used in above experiments, the HRTEM profile imaging in our study can observe the relaxation not only in first layer but also in the layers beneath the surface. Our HRTEM profile images reveal that the Zn ions inward and outward displacements in first and second layer were estimated around -13% $d_{(01\bar{1}0)} \approx 0.37$ Å and 17% $d_{(01\bar{1}0)} \approx 0.48$ Å, respectively and the in-plane movement of the Zn ions in surface is not detectable in our profile images. Our result on the displacement of Zn ions in the first layer has good agreement with the LEED results by Duke et al. [18] and the density-functional calculation by Meyer and Marx [25]. Due to the weak contrast of oxygen ions in HRTEM images, it is difficult to measure the displacement of oxygen ions directly from the HRTEM images. Based on the simulated results, two different relaxation cases on oxygen ions have been observed in our HRTEM profile images. There is no clear relaxation for the oxygen ions in Fig. 4. In addition, in Fig. 5, the relaxation on oxygen ions was confirmed. The best fitting HRTEM simulated image suggests the displacement of the oxygen ion in the first layer is around $-0.1d_{(01\bar{1}0)} + 0.1c$ and to the oxygen ions in the second layer is $\sim 0.1c$.

3.3. The $(0\bar{1}11)$ polar surface

The $(0\bar{1}11)$ is another polar surface of the wurtzite ZnO. Fig. 6a gives a HRTEM profile image of oxygen-terminated $(0\bar{1}11)$ polar surface. The head-to-tail arrangement of the dark rods directs the positive [0001] direction. Therefore, the inclined surface at the right-hand side should be the oxygen-terminated $(0\bar{1}11)$ polar surface. The positions of the Zn corresponded dark contrast centers at surface remain the right stacking sequence as extended from the quantum dot volume. Besides the dark rods, several weak rods pointed by arrowheads appear at the outmost layer. In order to find out what corresponds to this contrast, we carried out HRTEM image simulation. The atomic model of a perfect $(0\bar{1}11)$ polar surface is displayed

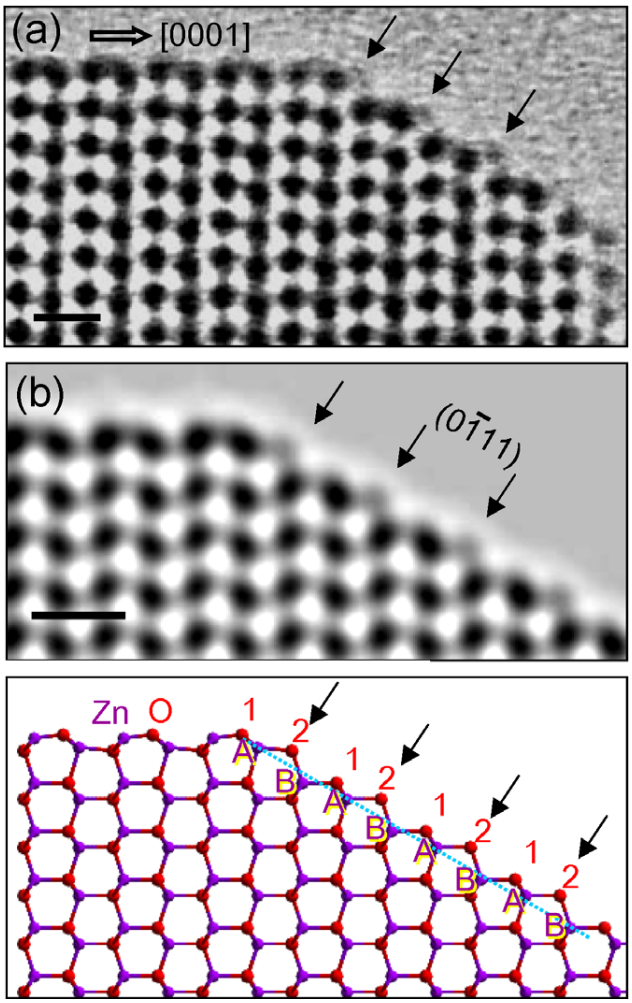

Fig. 6. (a) and (b) are experimental and simulated HRTEM profile images of the non-reconstructed, oxygen-terminated $(0\bar{1}11)$ polar surface. The atomic model used for the simulation is displayed in (c). The scale bars correspond to 5 Å.

in Fig. 6c. Although the surface is uniquely composed of oxygen ions, the oxygen ions at the surface can be divided into two groups, the oxygen ions in group "2" are pointed by arrowhead, oxygen ions in group "1" are those located in between the arrowheads (see Fig. 6c). The $[2\bar{1}\bar{1}0]$ projected distances between these oxygen ions with their nearest Zn ions are $0.3826c \approx 1.99$ Å (group 2) and $a/\sqrt{6} \approx 1.33$ Å (group 1). If there is no surface reconstruction, we are supposed to see the image of the oxygen ions belonging to group "2" at the surface in the HRTEM profile image, for the Zn–O distance is beyond the instrument resolution (of 1.7 Å). The simulated image based on the non-reconstructed surface model shown in Fig. 6c is displayed in Fig. 6b. The week rods pointed by arrowheads give the image of the oxygen ions. Comparing the simulated image in Fig. 6b with the experimental one in Fig. 6a, it is clear that the weak rods pointed by arrowheads in Fig. 6a correspond to the image of surface oxygen ions. The direct observation of the oxygen ion image, on

the other hand, reveals that there is no surface reconstruction occurred.

The projected length of the $(0\bar{1}1)$ polar surface in Fig. 6a is less than 3 nm, the surface reconstruction may be unnecessary for balancing the polar surface induced electrostatic energy due to the strong influence from the corners or edges. With expanding in surface area, the reconstruction of the $(0\bar{1}1)$ polar surfaces have been observed, as shown in Fig. 7a and b. The positive [0001] direction is identified following the rule discussed above. Then the inclined surfaces in Fig 7a and b are determined as oxygen-terminated $(0\bar{1}1)$ polar surfaces. Instead of the periodically zig-zag shaped non-reconstructed surface, the surfaces in Fig. 7a and b are rather flat.

A new phenomenon of the reconstructed surface is the regularly arranged dips, which are indicated by arrowheads. The distance between the two adjacent dips in Fig. 7b is twice of the size of the unit cell as shown in Fig. 6c. Thus, the new surface shown in Fig. 7b can be defined as a $\times 2$ reconstruction. In order to retrieve the relaxed positions of Zn and oxygen ions at the surface, several surface models have been built. The best-fitting one is displayed in Fig. 8. Taking the sample thickness as 21.66 Å and defocus −286.7 Å, the simulated HRTEM profile image is shown in Fig. 7c. Same as the surface oxygen ions, the Zn ions just beneath the exposed oxygen layer can also be divided into two groups based on the $[2\bar{1}\bar{1}0]$ projected Zn–O bonding distances. We use "A" and "B" to represent the Zn ions in Figs. 6c and 8.The Zn ions with shorter projected bonding distance belong to group "A", and the Zn ions with longer projected bonding distance belong to group "B". The reconstruction on the $(0\bar{1}1)$ polar surface is mainly related to the Zn ions of type B and its linked oxygen ions of type 2. If the type B Zn ion does not relax, the linked oxygen ion of type 2 will be displaced inward. If the oxygen ion of type 2 dose not shift, the connected Zn of type B will move outward. The real case in Fig. 7a and b is that the Zn ions are displaced inward every other one. Although small inward displacement of oxygen ions of type 1 was observed in Fig. 8, the displacement of type B Zn ions and type 2 oxygen ions is dominant. The outward displacement of Zn ions and the inward displacement of oxygen ions tend to minimize the electrostatic interaction energy introduced by the polar charges on the $(0\bar{1}1)$ surface.

It is important to note that only oxygen-terminated $(0\bar{1}1)$ polar surfaces were observed in our experiments. We did not find Zn-terminated $(01\bar{1}\bar{1})$ polar surface from the quantum dots. It may be related to its higher surface energy. To our knowledge, there is little study about the $\{0\bar{1}11\}$ polar surface reconstruction. Our HRTEM profile images of the $(0\bar{1}1)$ polar surface may help understanding of the growth mechanism of $\pm(0\bar{1}1)$ polar surface induced nanostructures, such as spring and helix shapes [47].

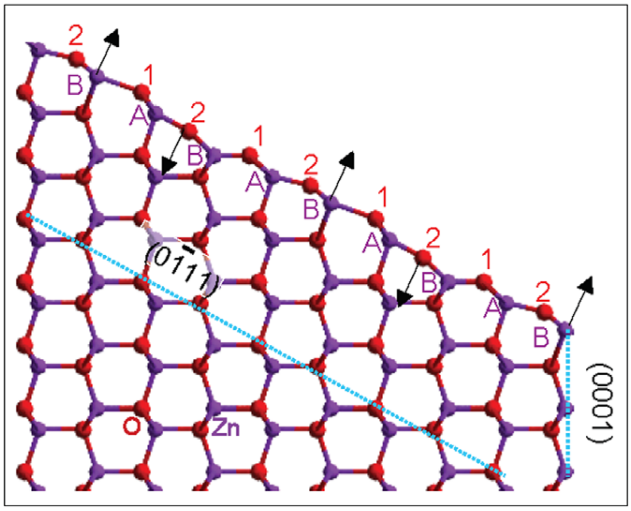

Fig. 8. Atomic model of the reconstructed, oxygen-terminated $(0\bar{1}1)$ polar surface.

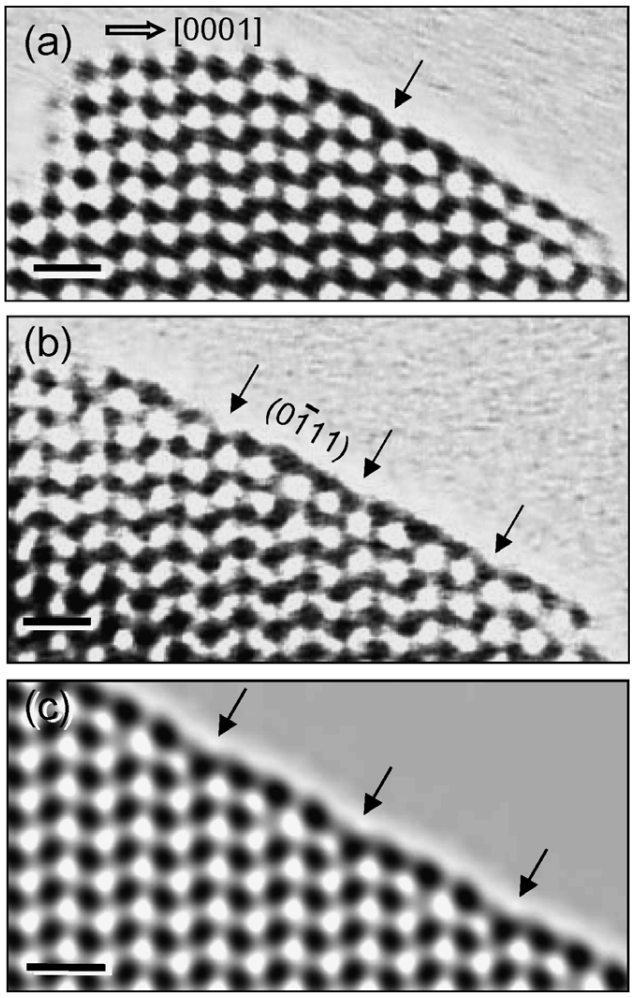

Fig. 7. (a), (b) and (c) are experimental and simulated HRTEM profile images of the reconstructed, oxygen-terminated $(0\bar{1}1)$ polar surface. The atomic model used for the simulation is displayed in Fig. 8. The scale bars correspond to 5 Å.

3.4. The ±(0001) polar surfaces

The faceted quantum dot in Fig. 9 gives the (0001) and $(000\bar{1})$ polar surfaces. Checking the head-to-tail arrangement of the dark rods, the top surface can be identified as Zn-terminated (0001) polar surface, while the bottom is the oxygen-terminated $(000\bar{1})$ polar surface. The $[2\bar{1}\bar{1}0]$ projected O–Zn bonding distance in the (0001) and $(000\bar{1})$ polar surfaces is around 1.33 Å for the non-reconstructed case, beyond the resolution of our instrument. Thus, we cannot distinguish the oxygen or Zn ions at the outmost surface layers. The contrast of short dark rods observed in HRTEM images contains the contributions from both oxygen and Zn ions. The contrast centers of the dark rods are picked up and represented by dots in Fig. 9b using the Gatan Digital Micrograph software. The *c*-plane inter-planar distance does not show relaxation. However, compared to the flat $(000\bar{1})$ polar surface, the dark centers of the rods for the (0001) polar surface may show a larger error bar.

Fig. 10 shows two other HRTEM profile images of Zn-terminated (0001) polar surface. The contrast centers of the Zn ion corresponded dark rods in Fig. 10a are reproduced in Fig. 10c. The contrast centers of the top layer have a larger height variation (around 0.7 Å), while in the second and third layers, the variation just between $0.1 \sim 0.3$ Å. Compared to the uniform contrast of the dark rods at $(000\bar{1})$-O polar surface, the contrast of the dark rods at (0001)-Zn polar surface displays a large difference.

It has also been found that the shape of the dark rods at the (0001)-Zn surface is different from that of the $(000\bar{1})$-O, as indicated by an arrowhead in Fig. 9a. More examples of such cases are presented in Fig. 10 as indicated by arrowheads, where the rod exhibits a longer tail for the (0001)-Zn surface, while the one on $(000\bar{1})$-O shows a rounded shape. We now use image simulation to find a possible clue for this difference.

We now assumed a few cases as presented below. At the surface point "1" in Fig. 11a, the Zn ion occupancy was decreased to 50%; at point "2" the Zn ions were shift outward for about 0.1*c*; at point "3", the overlapped Zn ions suffer different shifted amplitudes (outward) away from the ideal position; at point "4", the Zn ions were shift inward for about 0.1*c*; at point "5", oxygen ions move outward; at point "6", the Zn ions move inward while oxygen ions move outward. The simulated image for these models is displayed in Fig. 11b by taking the sample thickness as 2 nm and focus as −286.7 Å. It is obvious that the low occupancy can introduce weak contrast at area "1" in Fig. 11b. The contrast center is only sensitive to the shift of Zn, disregards the position of the oxygen (like the areas of "4", "5" and "6"). The overlapped Zn ions suffering from different outward displacement produces a longer tail in the rod contrast like the area "3" in Fig. 11. At the same time, the contrast center do not shift outward as much as the point "2" case. Thus, our data may suggest the "random" outward displacement of the Zn ions in the top layer. Furthermore, the variation of the contrast at outmost layer may indicate the existence of Zn vacancies at (0001) polar surface.

For the Zn-terminated (0001) surface, some experiments gave the evidence of the existence of the Zn vacancies [16,48], but some are not [49], The calculated displacement of the surface Zn ions was inward [25,27],

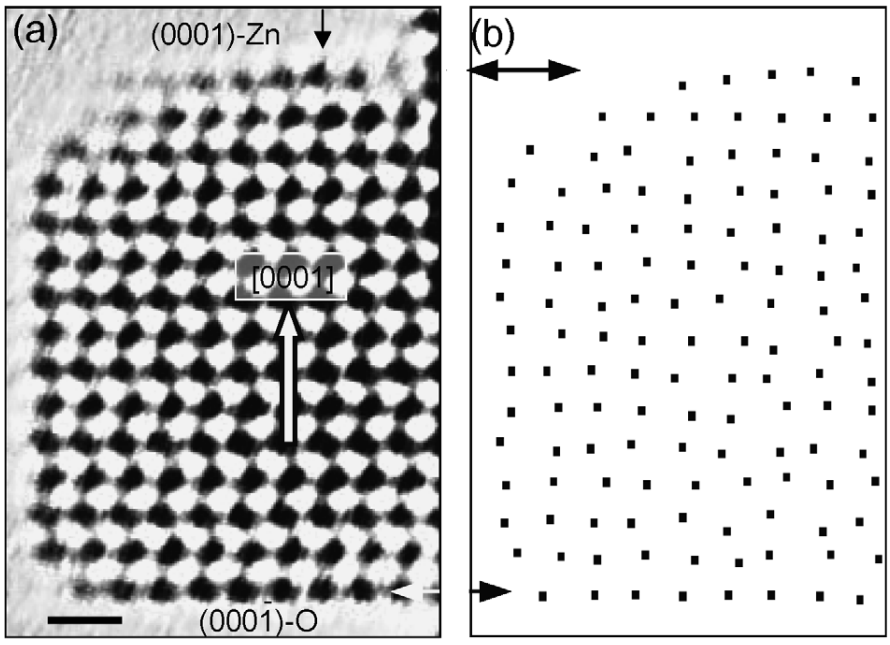

Fig. 9. HRTEM profile image (a) and the processed dark contrast center image (b) of a ZnO quantum dots. The top and bottom surfaces are the Zn-terminated (0001) and oxygen-terminated $(000\bar{1})$ polar surfaces, respectively. The scale bar corresponds to 5 Å.

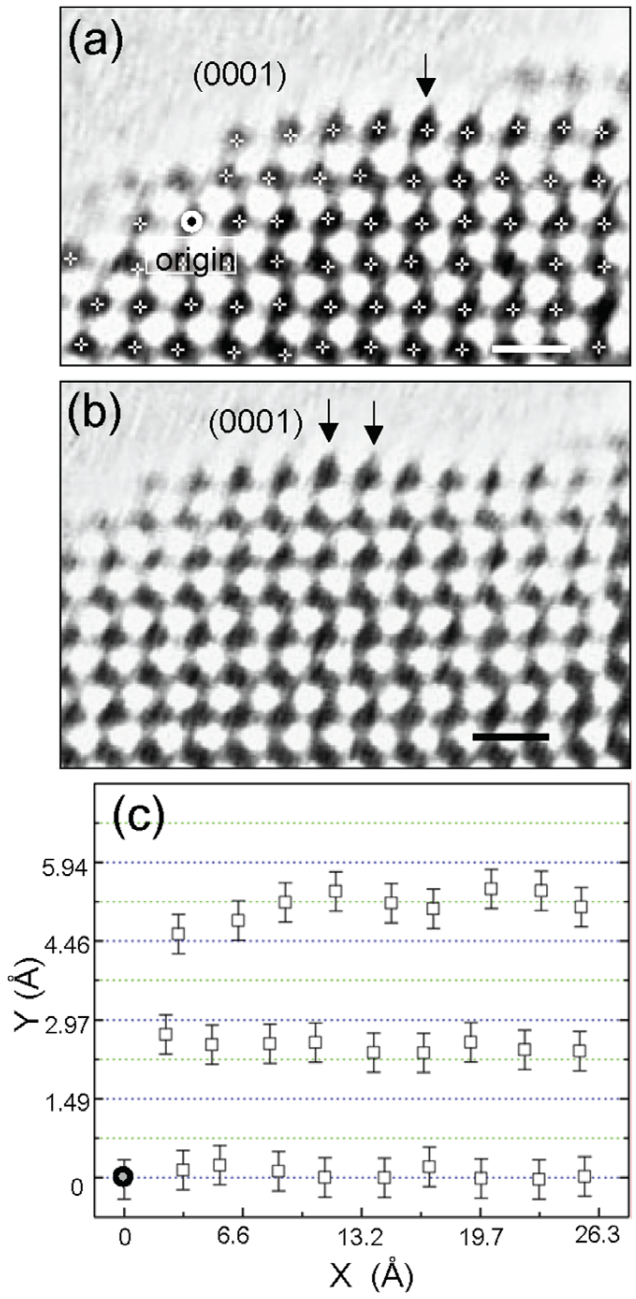

Fig. 10. (a) and (b) are two HRTEM profile images of Zn-terminated (0001) polar surface. The scale bars correspond to 5 Å. (c) Plot of the dark contrast centers in (a).

but the reported X-ray photo-diffraction [50] and coaxial impact-collision ion-scattering spectroscopy [31] suggested it is outward, which is consistent to our HRTEM result. Considering the three principal mechanisms [16] for the reduction in surface charge density as presented in the introduction section, the third mechanism of impurity atoms on the surface may not be the choice, for we grow ZnO quantum rod in TEM chamber in high vacuum condition and there are no detectable impurities. If the negative charges were transferred from O to Zn, the Zn ions

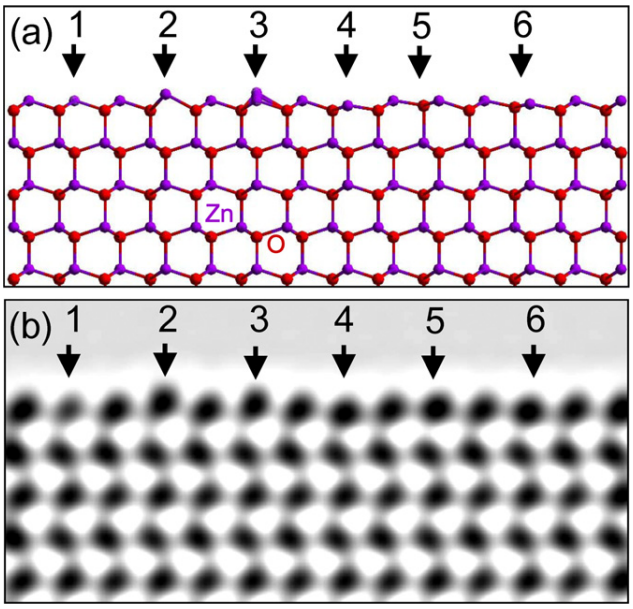

Fig. 11. Atomic model (a) and simulated image (b) to show the surface defects as labeled 1–6 (see text for details).

should take inward displacement, which is in contrast to our experimental result. The variation of the Zn ion contrast was observed in our HRTEM images, the mechanism based on removal of surface atoms is comparatively consistent to our experimental data. For the oxygen-terminated $(000\bar{1})$ surface, low-energy alkali-metal ion scattering (LEIS) did not observe clear surface relaxation [49] while surface X-ray diffraction revealed -0.24 ± 0.06 Å inward displacement of the surface oxygen ion [22]. Based on our HRTEM profile images, we cannot determine if there is an oxygen relaxation at the $(000\bar{1})$ polar surface, because it is impossible for us to separate the Zn and oxygen ions at surfaces. In addition, the contrast of oxygen ion is very weak in HRTEM profile images; therefore, there is a large measurement error when we face the profile images of $(000\bar{1})$ polar surface.

4. Summary

In this paper, using the profile imaging of high-resolution transmission electron microscopy (HRTEM), the surfaces of the small quantum dots of ZnO produced by irradiating a ZnO nanobelt in TEM have been studied. By comparing the observed image and the theoretically simulated images, the models of the surface structures are proposed. The main results are summarized as follows:

1. A technique has been demonstrated for identifying the positive and negative [0001] directions of ZnO directly from HRTEM images with electron beam along $[2\bar{1}\bar{1}0]$. This provides a lot of convenience for the identification of polar surfaces.

2. For the $(01\bar{1}0)$ non-polar surface, surface reconstruction has been observed. The Zn ions in the first and second layers have an inward ($\sim -13\%$ of $d_{(01\bar{1}0)}$) and outward ($\sim 17\%$ of $d_{(01\bar{1}0)}$) relaxation, respectively. The oxygen ions in the first and second surface layer prefer to shift towards vicinal Zn ions to shorten the bonding distance.
3. For the unreconstructed, oxygen-terminated $(0\bar{1}11)$ polar surface, the oxygen ions at the top layer have been directly imaged. In the reconstructed $(0\bar{1}11)$ surfaces, a $\times 2$ reconstruction has been identified and its structure model has been proposed.
4. The oxygen-terminated $(000\bar{1})$ polar surface shows no detectable reconstruction. For the Zn-terminated (0001) polar surface, our data may possibly indicate the existence of Zn vacancies in the surface and a random outward shift of the Zn ions.
5. Our data tend to support the mechanism of removal of surface atoms for maintaining the stability of (0001) polar surfaces.

Acknowledgements

The authors wish to thank Dr. C.L. Jia at Juelich research center, Germany for advice in image manipulation.

References

[1] Ü. Özgür, Ya.I. Alivov, C. Liu, A. Teke, M.A. Reshchikov, S. Doğan, V. Avrutin, S.-J. Cho, H. Morkoç, J. Appl. Phys. 98 (2005) 041301.
[2] J.B. Hansen, in: G. Ertl, H. Knoʊzinger, J. Weitkamp (Eds.), Handbook of Heterogeneous Catalysis, Wiley-VCH, Weinheim, 1997.
[3] F.-C. Lin, Y. Takao, Y. Shimizu, M. Egashira, J. Am. Ceram. Soc. 78 (1995) 2301.
[4] Z.L. Wang (Ed.), Nanowires and Nanobelts, Kluwer Academic Publisher, New York, 2003.
[5] J. Grabowska, A. Meaney, K.K. Nanda, J.-P. Mosnier, M.O. Henry, J.-R. Duclère, E. McGlynn, Phys. Rev. B 71 (2005) 115439.
[6] M. Law, L.E. Greene, J.C. Johnson, R. Saykally, P.D. Yang, Nature Mater. 4 (2005) 455.
[7] C. Yu, Q. Hao, S. Saha, L. Shi, X.Y. Kong, Z.L. Wang, Appl. Phys. Lett. 86 (2005) 063101.
[8] Z.L. Wang, J. Song, Science 312 (2006) 242.
[9] Z.L. Wang, X.Y. Kong, Y. Ding, P.X. Gao, W.L. Hughes, R. Yang, Y. Zhang, Adv. Funct. Mater. 14 (2004) 943.
[10] Z.W. Pan, Z.R. Dai, Z.L. Wang, Science 291 (2001) 1947.
[11] X.Y. Kong, Y. Ding, R. Yang, Z.L. Wang, Science 303 (2004) 1348.
[12] X.Y. Kong, Z.L. Wang, Nano Lett. 3 (2003) 1625.
[13] P.X. Gao, Z.L. Wang, Small 1 (2005) 945.
[14] P.X. Gao, Y. Ding, W.J. Mai, W.L. Hughes, C.S. Lao, Z.L. Wang, Science 309 (2005) 1700.
[15] JCPDS-80-0075, International centre for diffraction data (1999).
[16] O. Dulub, U. Diebold, G. Kresses, Phys. Rev. Lett. 90 (2003) 016102.
[17] R. Hoffmann, Rev. Mod. Phys. 60 (1988) 601.
[18] C.B. Duke, R.J. Meyer, A. Paton, P. Mark, Phys. Rev. B 18 (1978) 4225.
[19] W. Göpel, J. Pollmann, I. Ivanov, B. Reihl, Phys. Rev. B 26 (1982) 3144.
[20] N. Jedrecy, S. Gallini, M. Sauvage-Simkin, R. Pinchaux, Surf. Sci. 460 (2000) 136.
[21] C. Noguera, J. Phys.: Condens. Matter 12 (2000) R367.
[22] A. Wander, N.M. Harrison, J. Chem. Phys. 115 (2001) 2312.
[23] P.W. Tasker, J. Phys. C 12 (1979) 4977.
[24] R.W. Nosker, P. Mark, J.D. Levine, Surf. Sci. 19 (1970) 291.
[25] B. Meyer, D. Marx, Phys. Rev. B 67 (2003) 035403.
[26] A. Wander, F. Schedin, P. Steadman, A. Norris, R. McGrath, T.S. Turner, G. Thornton, N.M. Harrison, Phys. Rev. Lett. 86 (2001) 3811.
[27] J.M. Carlsson, Comput. Mater. Sci. 22 (2001) 24.
[28] I. Ivanov, J. Pollmann, Phys. Rev. B 24 (1981) 7275.
[29] J.E. Jaffe, N.M. Harrison, A.C. Hess, Phys. Rev. B 49 (1994) 11153.
[30] C.B. Duke, D.E. Lessor, T.N. Horsky, G. Brandes, K.F. Canter, P.H. Lippel, A.P. Mills Jr., A. Paton, Y.R. Wang, J. Vac. Sci. Technol. A 7 (1989) 2030.
[31] H. Maki, N. Ichinose, N. Ohashi, H. Haneda, J. Tanaka, Surf. Sci. 457 (2000) 377.
[32] C.B. Duke, A.R. Lubinsky, S.C. Chang, B.W. Lee, P. Mark, Phys. Rev. B 15 (1977) 4865.
[33] R. Dorn, H. Lüth, M. Büchel, Phys. Rev. B 16 (1977) 4675.
[34] M. Kunat, St. Gil Girol, Th. Becker, U. Burghaus, Ch. Wöll, Phys. Rev. B 66 (2002) 081402.
[35] O. Dulub, L.A. Boatner, U. Diebold, Surf. Sci. 519 (2002) 201.
[36] V. Staemmler, K. Fink, B. Meyer, D. Marx, M. Kunat, S. Gil Girol, U. Burghaus, Ch. Wöll, Phys. Rev. Lett. 90 (2003) 106102.
[37] B. Mayer, D. Marx, Phys. Rev. B 69 (2004) 235429.
[38] P.J. Moller, S.K. Komolov, E.F. Lazneva, J. Phys.: Condens. Matter 11 (1999) 9581.
[39] J.M. Gibson, M.L. McDonald, F.C. Unterwald, Phys. Rev. Lett. 55 (1985) 1765.
[40] Ping Lu, David J. Smith, Phys. Rev. Lett. 59 (1987) 2177.
[41] Ping Lu, David J. Smith, Surf. Sci. 254 (1991) 119.
[42] J.M. Cowley, A. Moodie, Acta Cryst. 10 (1957) 609.
[43] Z.L. Wang, X.Y. Kong, J.M. Zuo, Phys. Rev. Lett. 91 (2003) 185502.
[44] Y. Ding, C. Ma, Z.L. Wang, Adv. Mater. 16 (2004) 1740.
[45] Y.R. Wang, C.B. Duke, Surf. Sci. 192 (1987) 309.
[46] L. Whitmore, A.A. Sokol, C.R.A. Catlow, Surf. Sci. 498 (2002) 135.
[47] R. Yang, Y. Ding, Z.L. Wang, Nano Lett. 4 (2004) 1309.
[48] N. Jedrecy, M. Sauvage-Simkin, R. Pinchaux, Appl. Surf. Sci. 162–163 (2000) 69.
[49] S.H. Overbury, P.V. Radulovic, S. Thevuthasan, G.S. Herman, M.A. Henderson, C.H.F. Peden, Surf. Sci. 410 (1998) 106.
[50] M. Sambi, G. Granozzi, G.A. Rizzi, M. Casari, E. Tondello, Surf. Sci. 319 (1994) 149.